JOURNAL OF CATALYSIS 144, 1–8 (1993)

Increased Catalytic Activity Caused by Local Destruction of Linear Zeolite Channels: Effect of Reduction Temperature on Heptane Conversion over Platinum Supported in H-Mordenite

BRIAN T. CARVILL, BRUCE A. LERNER, BRADLEY J. ADELMAN, DOUGLAS C. TOMCZAK, AND WOLFGANG M. H. SACHTLER[1]

V. N. Ipatieff Laboratory, Center for Catalysis and Surface Science, Northwestern University, Evanston, Illinois 60208

Received May 6, 1993

The conversion of *n*-heptane was studied on Pt/HMor. The response of catalytic activity and isomerization selectivity to reduction temperature and metal dispersion is contrary to that known for Pt on amorphous supports or on zeolites with three-dimensional pore systems: samples reduced at 500°C, though having distinctly lower Pt dispersion, are about twice as active as samples reduced at 350°C. It is shown that for strictly one-dimensional pores the conditions of *single file diffusion* are fulfilled; products formed deep in the pores are unable to escape. Reduction at 500°C produces Pt particles large enough to locally destroy the zeolite; this transformation of one-dimensional into three-dimensional pores removes the transport restrictions of single file diffusion and increases site accessibility. © 1993 Academic Press, Inc.

INTRODUCTION

Bifunctional catalysts consisting of transition metal particles supported on an acidic support are important materials in view of their ability to isomerize linear alkanes (*1*, *2*). In the reaction network, acid sites are responsible for generating carbenium ions which undergo skeletal rearrangement (*3*, *4*); metal sites are instrumental in establishing alkane/alkene equilibration and limiting deactivation of the catalyst (*5*). The kinetic laws by which the rate constants of individual steps and the diffusion through pores are combined in a reaction network are basically similar for porous amorphous supports and crystalline zeolites with a three-dimensional system of channels.

Different phenomena are, however, predicted for zeolites with narrow *one-dimensional* channels. Molecular traffic in such pores is subject to rules that are not described by the familiar models of pore diffusion control as given by the Thiele modulus (*6*) and the Wheeler equation (*7*). For pore diameters on the order of the kinetic diameter of the reactants and products the reaction products can leave a site in the interior of a one-dimensional channel only if no other molecules block the space between reaction site and pore mouth (*8*). Under these severe transport limitations, the only reaction products that are observable are those generated at active sites near the pore mouths; any products formed deep in the pores are trapped.

The present study makes use of the isomerization of *n*-heptane on Pt/H-mordenite to focus on the specific changes in reaction kinetics which occur when a one-dimensional pore system is partially converted to a three-dimensional system by local destruction of the zeolite matrix. This is dependent on the size of the metal particles which can be varied by changing the reduction temperature and the metal loading. The proposed effects of particle growth and subsequent structural collapse are documented

[1] To whom correspondence should be addressed.

0021-9517/93 $5.00
Copyright © 1993 by Academic Press, Inc.
All rights of reproduction in any form reserved.

using transmission electron microscopy (TEM), CO chemisorption, and X-ray diffraction (XRD).

EXPERIMENTAL

Catalyst preparation. Two metal loaded samples were prepared: (1) 0.9 wt% Pt/HMor and (2) 5 wt% Pt/HMor. The blank zeolite, HMor, was prepared by washing 50 g of mordenite (LZ-M-8, UOP) with 10.97 g NH_4NO_3 (3× excess) in 2000 ml doubly deionized water. The pH of the solution was raised to 7.2 by adding dilute NH_4OH. The zeolite slurry was stirred for 24 h filtered, and air dried.

Ion exchange was performed by adding a dilute solution of Pt $(NH_3)_4^{2+}$ dropwise into a slurry containing NH_4Mor in doubly deionized water (200 ml/g) at room temperature (RT) over 24 h. The platinum/zeolite slurry was stirred for an additional 48 h. The sample was then filtered, washed with ~2000 ml of doubly deionized water, and air dried. In order to keep the samples in a fully hydrated state, the catalysts were stored in a saturator containing a saturated NH_4Cl solution.

Calcination. All samples were first calcined under a high flow (>2000 ml/min-g cat) of Linde UHP oxygen in a packed-bed reactor at atmospheric pressure. The temperature was ramped at 0.5°C/min from RT to 510°C and held at 510°C for 2 h. The sample was then purged at 510°C with Linde UHP argon or helium (>50 ml/min) for 20 min before cooling to RT. In this calcination step, the NH_4^+ ions are converted into H^+ ions, and the NH_3 ligands on the metal complex are oxidatively decomposed.

Reduction. Reduction was performed *in situ* on the reaction system. The samples were reduced in flowing Linde UHP hydrogen (20 ml/min) at atmospheric pressure. The temperature was ramped from RT to the reduction temperature (T_r) at 8°C/min and held at T_r for 30 min. Two reduction temperatures (350°C and 500°C) were used in this study. After reduction, the temperature was lowered to the reaction temperature (200°C).

Conversion of n-heptane. Four samples were tested for the conversion of *n*-heptane: 0.9% Pt/HMor (T_r = 350°C), 0.9% Pt/HMor (T_r = 500°C), 5% Pt/HMor (T_4 = 350°C), and 5% Pt/HMor (T_r = 500°C). The *n*-heptane (Aldrich, HPLC grade) was introduced to the reactor by flowing hydrogen (20 ml/min) through a saturator filled with n-heptane at 10°C; this corresponds to an *n*-heptane vapor pressure of 20.5 Torr. All reactions were carried out at 200°C and 1 atm, and the catalyst charge for each run was 100 mg. The reaction was monitored with an online HP 5790A gas chromatograph equipped with a cross-linked methyl silicone capillary column and a flame ionization detector (FID). Injections were made at 10 min time on stream (TOS), and then every 30 min for 3 h. Steady state was reached after approximately 1 h TOS.

Transmission electron microscopy. Electron micrographs were made with a Hitachi HF-2000 high-resolution analytical electron microscope (HRAEM) equipped with a field emission gun electron source and operated at 200 kV. Images were made in the bright field mode and were collected with suitable aperture and exposure time to minimize beam damage to the zeolite. Catalyst samples were powders and were dispersed onto "holey carbon" coated grids which were then introduced to the microscope column which was evacuated to less than 1×10^{-6} Torr.

X-ray diffraction. X-ray powder diffraction data were collected using a Rigaku Geigerflex diffractometer using a CuK_α source and a Ni filter. Scans were run between 15 and 40°2Θ at 0.05°2Θ to determine line broadening for major peaks.

CO chemisorption. Chemisorption measurements were made using a conventional vacuum system at room temperature (23°C). After calcination and reduction, the sample was purged at the reduction temperature in UHP He for 10 min, and then evacuated to less than 5×10^{-6} Torr for 30 min. The

manifold was filled with the desired pressure of CO, which was then expanded into the reactor. The initial and equilibrium pressures of CO were monitored using a Setra 360 digital pressure gauge; isotherms were measured between 0–100 Torr. After the first isotherm was measured, the sample was evacuated to less than 3×10^{-5} Torr for 15 min, and a second isotherm was measured. Following the second isotherm, the sample was again evacuated to less than 3×10^{-5} Torr, and the volume of the reactor was determined by expanding UHP He from the manifold into the reactor. The amount of chemisorbed CO was determined by extrapolating the isotherms to zero pressure, and then taking the difference between the first and second isotherms.

RESULTS

Figure 1 shows TEM photographs for the two extreme conditions: (a) 0.9% Pt/HMor, T_r = 350°C, and (b) 5% Pt/HMor, T_r = 500°C. From previous studies, we expect that the Pt particles will increase in size as metal load and reduction temperature are increased (*9, 10*). This assertion is confirmed by these data. The photograph in Fig. 1a has a higher magnification than the one in Fig. 1b; no Pt particles are visible, even though the lattice fringes of the zeolite framework can clearly be seen. The resolution of this microscope is 7 Å, thus defining an upper limit of the Pt particle size. In Fig. 1b (high metal load, high reduction temperature), the scale is much larger and black images indicating Pt particles can be resolved. These particles appear to be well dispersed and inside the zeolite; their sizes are between 10 and 15 Å.

The results from the CO chemisorption experiments are shown in Table 1. As the reduction temperature is increased from 350°C to 500°C, the CO/Pt ratio decreases from 0.95 to 0.61 for the 0.9% Pt/HMor and 0.76 to 0.57 for the 5% Pt/HMor. These results confirm that as the reduction temperature or the metal load is increased, the size of the metal particles in the zeolite increases.

Figure 2 shows a comparison of the steady state activity for the Pt/HMor with two different loadings (0.9 and 5%) and two reduction temperatures (350 and 500°C). The activity of the sample containing 5% Pt is greater than the activity for the samples containing 0.9% Pt; this difference in activity is not proportional to the increase in metal in the sample. For both catalysts, the activity doubles when the reduction temperature is increased to 500°C.

One measure of catalyst deactivation is the ratio of the steady-state activity to the initial activity. Figure 3 shows this ratio for the two samples treated at the low and high reduction temperature. The samples reduced at higher temperature deactivate less than those reduced at low temperature. This is true regardless of the metal load. One might have expected that the samples with higher metal dispersion would be more effective at removing coke precursors; however, this is not the case.

Figure 4 shows the percentage of *n*-heptane isomerization. The balance of the product distribution is cracking products (primarily C_3's and C_4's). At high reduction temperatures, the isomerization selectivity increases. However, the relative amount of multiple-branched isomers decreases with increasing metal load and reduction temperature (Fig. 5).

XRD was used to determine if the zeolite shows any loss of crystallinity accompanying the growth of the Pt particle in the mordenite pore. Figure 6 shows the XRD patterns for (a) 5% Pt/HMor, T_r = 350°C, and (b) 5% Pt/HMor, T_r = 500°C, and (c) the difference (a − b). The width of the peaks (FWHM) for the sample reduced at 350°C is 0.25°2Θ, while the width of the peaks for the sample reduced at 500°C is 0.30°2Θ. The dip–peak–dip pattern in Fig. 6c is a fingerprint for an increase in peak width; a peak shift would be observed as a dip–peak pattern. This increase in XRD peak width is evidence for a decrease in

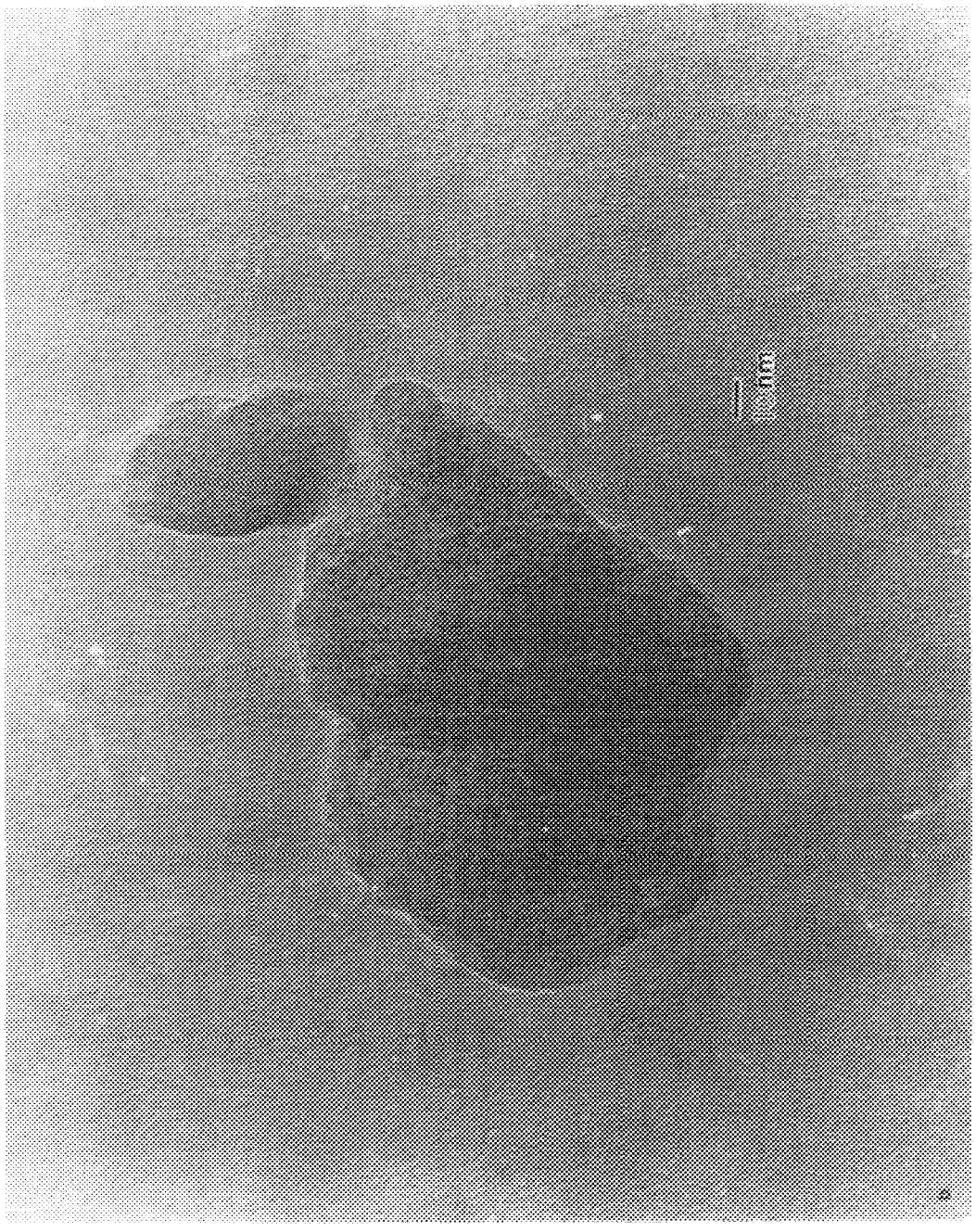

FIG. 1. Transmission electron micrographs of (a) 0.9% Pt/HMor (T_c 510°C, T_r 350°C) and (b) 5% Pt/HMor (T_c 510°C, T_r 500°C).

TABLE 1

CO/Pt Ratios

	T_r 350°C	T_r 500°C
0.9% Pt/HMor	0.95	0.61
5% Pt/HMor	0.76	0.57

zeolite crystallinity after reduction at 500°C. No decrease in crystallinity was observed with a metal-free zeolite that was given the same treatment.

DISCUSSION

The CO chemisorption and the TEM results clearly show that the Pt particles are larger after reduction at 500°C than after reduction at 350°C. This is in agreement with general experience concerning the effect of reduction temperature on particle growth. In the conventional view of bifunctional catalysis, one would expect that the overall activity decreases with decreasing amount of exposed metal (*11*, *12*). Moreover, one would expect that the selectivity shifts towards multiple branched products, because the contact time of unsaturated intermediates with acid sites becomes larger when the number ratio of metal sites/acid sites decreases (*13*). The results of the present research are contrary to both expectations: the data show that, as the metal dispersion decreases, the activity of the bifunctional catalyst *increases* and selectivity shifts towards *monobranched* products.

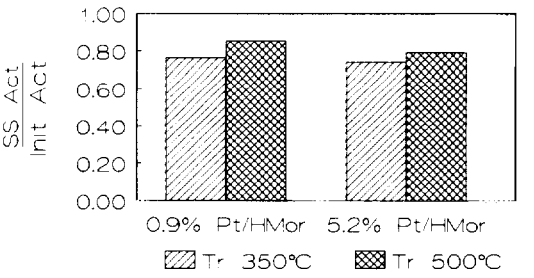

FIG. 3. Effect of the reduction temperature and metal load on the deactivation of Pt/HMor.

The results are, however, in good agreement with an alternate model which is applicable to metals supported on materials such as mordenite with narrow one-dimensional channels. This model has been described in detail by Kärger *et al.* (*8*); it was successfully applied by Lei *et al.* to the catalysis of Pt supported in mordenite (*10*) and by Karpiński *et al.* to the catalysis of Pd on another support with narrow one-dimensional pores, viz., zeolite L (*14*).

The essence of the model is that *single file diffusion* determines transport in one-dimensional pores which are wide enough for molecules to enter, but too narrow for simultaneous diffusion of inbound reactant molecules and counterdiffusion of outbound products. Under those conditions of temperature and pressure which lead to a high crowding of the pores with physisorbed molecules in the steady state of the reaction,

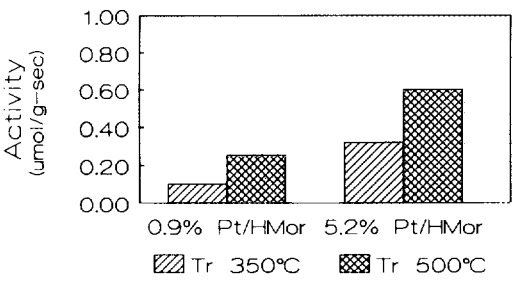

FIG. 2. Effect of reduction temperature and metal load on the steady-state activity of Pt/HMor for *n*-heptane conversion.

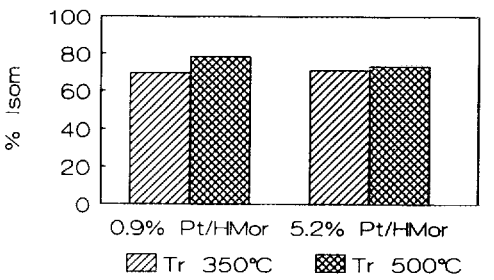

FIG. 4. Effect of the reduction temperature and metal load on the isomerization selectivity of Pt/HMor.

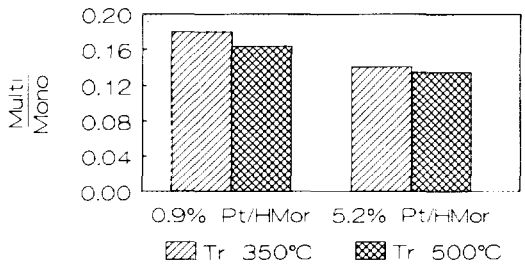

FIG. 5. Effect of the reduction temperature and metal load on the multiple-branched/monobranched ratio of *n*-heptane isomers.

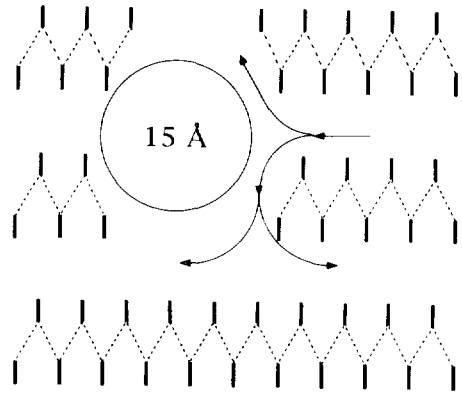

FIG. 7. Schematic showing the transformation of a one-dimensional channel to a three-dimensional channel by a growing metal particle.

catalyst activity is no longer controlled by the *density*, but by the *accessibility* of the active sites.

The uptake of various hydrocarbons in mordenite was extensively studied by Eberly (*15*). From his data, it is possible to determine the equilibrium uptake of *n*-hexane in mordenite at 200°C and 20 Torr (the conditions used in the *n*-heptane reaction study). Based on the calculated concentration, the intermolecular spacing of *n*-hexane within the pores of mordenite is 12 Å. As the heat of adsorption is known to increase with the length of the carbon chain, it is reasonable to assume that under the present conditions the pores will become even more crowded with n-heptane.

The three criteria for single file diffusion have therefore been met: one-dimensional pores, difficulty of counter-diffusion in the pore, and molecular crowding. To explain the observed changes in activity, we propose that the growth of the metal particles during reduction to 500°C is accompanied by local destruction of the zeolite. This zeolite destruction is confirmed by a loss in crystallinity as measured by XRD. A similar destruction by the growth of metal particles inside Y zeolite has been recently reported (*16–18*). Local collapse of the mordenite would locally convert its one-dimensional pore system into a three-dimensional system (see Fig. 7). This increases the accessibility of the active sites to molecules in the gas phase, and accounts for the observed increase in activity. Because the local destruction occurs in the vicinity of the metal particles, an increase in the metal function of the catalyst is expected. The increase in monobranched products and decrease in deactivation for samples reduced at high temperature are consistent with this increase in metal function.

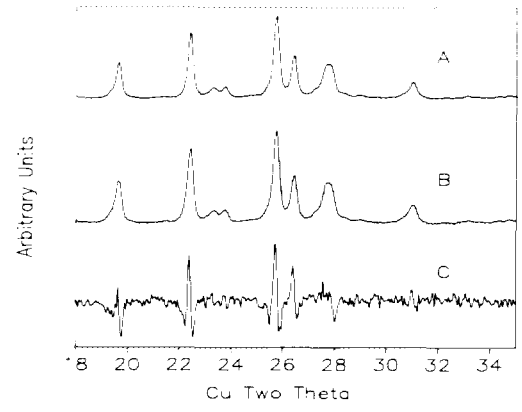

FIG. 6. Effect of reduction temperature on the XRD patterns of 5% Pt/H/Mor: (a) T_r 350°C, (b) T_r 500°C, and (c) a − b.

CONCLUSIONS

An inverse effect of reduction temperature on catalytic activity is observed. Pt/HMor samples reduced at 500°C have twice the activity for n-heptane isomerization as

samples reduced at 350°C. In addition, shifts in selectivity (more monobranched hexanes, less deactivation) indicate that the metal function of the catalyst has increased at high reduction temperatures. We believe that these phenomena are the result of disrupting a mass transport limitation called single file diffusion. Because of the linear pores and the large amount of hydrocarbons absorbed in the pores, the observed product distributions stem from sites near the pore mouth. However, when large metal particles are formed, local collapse of the zeolite occurs, creating a three-dimensional pore system. This increase in dimensionality increases the accessibility of gas phase molecules to the inside of the zeolite. It is this increase in accessibility, and not changes in the metal dispersion, that dominate the observable reaction kinetics.

ACKNOWLEDGMENTS

The authors acknowledge AKZO Corporate Research America for funding and Professor V. Dravid for the use of his laboratory in making electron micrographs. BTC also acknowledges financial support in the form of an NSF graduate student fellowship.

REFERENCES

1. Kouwenhoven, H. W., van Zijll Langhout, W. C., *Chem. Eng. Prog.* **67,** 65 (1971).
2. Kouwenhoven, H. W., *in* "Molecular Sieve Zeolites," A.C.S. Advan. Chem Ser., Vol 121, p. 529. Am. Chem. Soc., Washington, DC, 1973.
3. Brouwer, D. M., *in* "Chemistry and Chemical Engineering of Catalytic Processes" (R Prins and G. C. A. Schuit, Eds.), NATO ASI Ser. E., No 39., p. 137. Rockville, Sijthoff and Noordoff, 1980.
4. Pines, H., and Haag, W., *J. Am. Chem. Soc.* **82,** 2471 (1960).
5. G. A. Mills, H. Heinemann, T. H. Milliken, and A. G. Oblad, *Ind. Eng. Chem.* **45,** 134 (1953).
6. Thiele, E. W., *Ind. Eng. Chem.* **31,** 916 (1939).
7. Froment, G. F. and Bischoff, K. B., *in* "Chemical Reactor Analysis and Design," p. 164. Wiley, New York, 1990.
8. Kärger, J., Petzold, M., Pfeiffer, H., Ernst, S., and Weitkamp, J., *J. Catal.* **136,** 283 (1992).
9. Lerner, B. A., Carvill, B. T., and Sachtler, W. M. H., *J. Mol. Catal.* **77,** 99 (1992).
10. Lei, G. D., and Sachtler, W. H. H., *J. Catal.* **140,** 601 (1993).
11. F. Ribeiro, C. Marcilly, M. Guisnet, E. Freund, H. Deiput, *in* "Catalysis by Zeolites" (B. Imelik *et al.*, Eds.), p. 319. Elsevier, Amsterdam, 1980.
12. Ribeiro, F., Marcilly, C., and Guisnet, M., *J. Catal.* **78,** 275 (1982).
13. Guisnet, M., Alvarez, F., Gianetto, G., and Perot, G., *Catal. Today* **1,** 415 (1987).
14. Karpiński, Z., Gandhi, S., and Sachtler, W. M. H., *J. Catal.*, **141,** 337 (1993).
15. Eberly, P. E., *J. Phys. Chem.* **67,** 2404 (1963).
16. Jaeger, N. I., Rathousky, J., Schulz-Ekloff, G., Svenson, A. and Zukal, A., *in* "Zeolites: Facts, Figures, Future" (P. A. Jacobs and R. A. van Santen, Eds.), p. 1005. Elsevier, Amsterdam, 1989.
17. Jaeger, N. I., Jaeger, A. L. and Schulz-Ekloff, G., *J. Chem. Soc. Faraday Trans.* **87(8),** 1251 (1991).
18. Sachtler, W. M. H., Zhang, Z., Stakheev, A. Y., and Feeley, J. S., *in* "New Frontiers in Catalysis" (L. Guzci, F. Solymosi, and P. Tetenyi, Eds.), p. 271. Akademiai Kiado, Budapest, 1993.